Proceedings of the 20th International Conference on Soil Mechanics and Geotechnical Engineering– Rahman and Jaksa (Eds)

Large deformation finite element analysis to predict penetration resistance of offshore pipelines

Analyse par éléments finis à grande déformation pour prédire la résistance à la pénétration des pipelines offshore

Samanthika Liyanapathirana
School of Engineering, Design and Built Environment, Western Sydney University, Australia
s.liyanapathirana@westernsydney.edu.au

ABSTRACT: This paper presents an investigation into the penetration resistance of offshore pipelines during initial vertical penetration and subsequent lateral movement due to lateral buckling or submarine landslides. Since the soft seabed deformations are large during the penetration process, this problem cannot be simulated using a small-strain finite element analysis. Therefore, a Large Deformation Finite Element (LDFE) analysis procedure has been developed using the PYTHON language to simulate this problem utilising the features within the ABAQUS/Standard finite element modelling program. A coupled analysis considering excess pore pressure generation and subsequent dissipation has been performed for the pipeline penetration problem. Results from the LDFE analysis was compared with existing solutions and data collected from centrifuge tests carried out at the National Geotechnical Centrifuge Facility at the University of Western Australia to validate the proposed new modelling procedure.

RÉSUMÉ : Cet article présente une étude de la résistance à la pénétration des pipelines offshore lors de la pénétration verticale initiale et du mouvement latéral subséquent dû au flambage latéral ou aux glissements de terrain sous-marins. Puisque les déformations molles du fond marin sont importantes pendant le processus de pénétration, ce problème ne peut pas être simulé en utilisant une analyse par éléments finis à petite déformation. Par conséquent, une procédure d'analyse par éléments finis à grande déformation (LDFE) a été développée à l'aide du langage PYTHON pour simuler ce problème en utilisant les fonctionnalités du programme de modélisation par éléments finis ABAQUS/Standard. Une analyse couplée tenant compte de la génération de pression interstitielle excessive et de la dissipation subséquente a été effectuée pour le problème de pénétration du pipeline. Les résultats de l'analyse LDFE ont été comparés aux solutions existantes et aux données recueillies lors d'essais de centrifugation effectués à la National Geotechnical Centrifuge Facility de l'Université d'Australie occidentale pour valider la nouvelle procédure de modélisation proposée.

KEYWORDS: Offshore pipelines, Large Deformation Finite Element Analysis, penetration resistance, failure mechanism.

1 INTRODUCTION

In deep water, offshore pipelines are laid over seabed directly without any additional restraining mechanisms or trenching. During the laying process, they embed shallowly over the seabed predominantly due to the self-weight. However, pipelines will over embed due to dynamic lay effects and stress concentration at the touchdown location. In addition, forces due to wave action and pipe laying equipment may also contribute to the initial positioning. Geotechnical design of pipelines is underdeveloped compared to other common foundation types but an area of ongoing research. There has been significant work over the last decade with a large body of published research and several design codes. At the same time, pipeline design is distinctly different to other foundation types because lateral deformations expected of pipelines during service are relatively large compared to other foundation types such as piles or footings. In general, lateral deformations of pipelines are equivalent to few diameters of the pipeline and often they can exceed more than ten pipe diameters across the seabed. However, for other foundation types, lateral deformations are only a fraction of the foundation diameter. Therefore, pipeline design should consider resistance to both vertical penetration and lateral deformations.

Classical plasticity theory has been widely used to investigate the failure mechanisms and ultimate loads during pipe penetration into the seabed (e.g., Martin and Randolph, 2006; Randolph and White, 2008). Also finite element analysis has been widely used to study this problem considering small-strain (e.g., Aubeny et al., 2005; Merifield et al., 2008, 2009) and large deformation (e.g., Chatterjee et al., 2012; Wang et al., 2010) analysis approaches. Centrifuge test data published by Dingle et al. (2008) are extremely useful as a validation tool for researchers who work in this area using either numerical modelling or developing analytical solutions.

When using small-strain based finite element modelling, it is not possible to simulate penetration of the pipeline from the surface of the seabed. Always analysis was carried out considering a wished-in-place pipeline. Recently published research considering Large Deformation Finite Element (LDFE) analysis by Wang et al. (2010) and Chatterjee et al. (2012), strain softening of the soil and rate effects are incorporated but their analysis procedures are not capable of capturing the pore pressure effects.

When a pipeline is laid over the seabed, excess pore pressures will generate. Hence, it is important to understand how excess pore pressures will influence the resistance to lateral pipeline deformations. Therefore, in this paper, a coupled LDFE analysis has been proposed incorporating the pore pressure effects to simulate the pipeline penetration and subsequent lateral deformations in the soft seabed. First part of the paper presents the development of the LDFE analysis procedure using the PYTHON development environment within the ABAQUS/Standard finite element program. In the second part, the results for penetration resistance during vertical penetration are compared with the centrifuge test data by Dingle et al. (2008), LDFE analysis results by Wang et al. (2010) and Upper Bound (UB) solution by Randolph and White (2008). Finally, the capability of the proposed approach in analysing combined large vertical and lateral penetrations, which cannot be simulated using a traditional small-strain based finite element programs (e.g., ABAQUS/Standard, PLAXIS, PHASE 2&3) is demonstrated.

2 LDFE ANALYSIS PROCEDURE

The LDFE analysis procedure presented in this paper is written by the author using the PYTHON Development Environment (PDE) within the ABAQUS/Standard finite element modelling program. The analysis is carried out in a series of small-strain finite element analysis stages. ABAQUS/Standard input file for each analysis was created using the PYTHON code developed by the author. After each analysis, the deformed boundary of the mesh is captured and a new mesh is generated. The new mesh can have either the same number of elements or it can be changed.

All variables corresponding to integration points and nodes of the old mesh were transferred to the new mesh using the solution mapping algorithm in ABAQUS/Standard. During solution mapping, all variables corresponding to integration points of the old mesh are transferred to nodes of the old mesh and averaged when a node is shared by several elements. Then the interpolation is carried out to the integration points of the new mesh. Similarly, all nodal variables such as pore pressures in a coupled analysis are transferred from nodes of the old mesh to the nodes of the new mesh. The variables transferred from the old mesh to the new mesh will act as initial conditions for the new mesh.

The duration of each analysis should be determined by taking into account the mesh deformations, because the accuracy of analysis depends on the mesh deformations at the end of each remeshing step. Therefore, the criteria for the generation of the new mesh using the boundary of the deformed old mesh should be set before excessive mesh deformations. If there is a discontinuity in the solution, it can be due to the use of a too coarse mesh or carrying out remeshing, when the elements are excessively distorted. Specific details regarding the LDFE approach presented in this paper will be discussed in the following sections.

3 NUMERICAL MODEL

The problem presented in this paper is about pipeline penetration. Since the length of the pipeline is significantly larger than the diameter, problem is simulated using a two-dimensional plane-strain model as shown in Figure 1. Since the simulation involves vertical penetration and subsequent lateral movement of the pipeline, symmetry in geometry has not been considered when creating the finite element mesh.

The soil domain, which represents the seabed in this case, extends sufficiently away from the pipeline, avoiding any boundary effects on measured penetration resistance. The model shown in Figure 1 extends 17.5D in the horizontal direction and 6.25D in the vertical direction, where D is the diameter of the pipeline. The two side edges of the model were restricted to move in the horizontal direction but freed to move in the vertical direction. The bottom boundary was restrained in both vertical and horizontal directions.

The pipe was modelled as an elastic material with a very high Young's modulus compared to the soil to avoid any deformations. The seabed is modelled assuming the Mohr-Coulomb failure criteria. Material properties for both seabed and pipeline are given in Table 1, where seabed properties correspond to drained properties. The Pipeline was modelled using the element CPE4, which is a four-node quadrilateral element. The soil was modelled with the same element but with pore pressure degrees of freedom at the corner nodes, CPE4P. Although CPE4 is a linear element, for the remeshing analysis, linear element could avoid convergence issues faced with the quadratic CPE8R and CPE8RP elements, and CPE8 and CPE8P elements.

The pipe-soil interaction was modelled using the contact algorithm in ABAQUS/Standard with soil surface as the slave surface and the pipe surface as the master surface. Interaction was modelled using the penalty approach. Different options available within the penalty approach when defining interface friction will be discussed in Section 4.

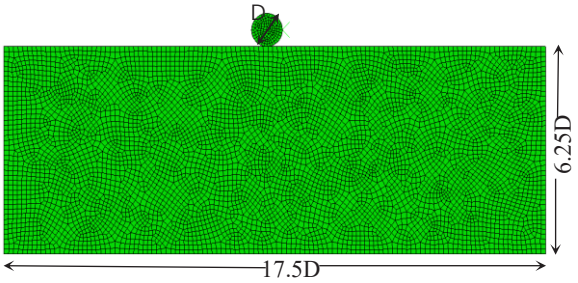

Figure 1. Finite element model

All the analyses presented in this paper are performed based on the principal of effective stresses considering the pore pressure generation and dissipation. Water table is assumed to be at the surface and simulated using a zero pore pressure boundary in the finite element model.

Pipeline penetration in both vertical and lateral drections were simulated at a rate of 1 mm/s. The vertical penetration was carried out for a depth equivalent to one diameter and the lateral movement was also simulated up to a distance of one diameter. For each case presented in this paper, 20 remeshing analyses were performed, with 10 in each direction. That means each analysis simulated a penetration of 10% of D in respective direction.

Initial and each remeshing analysis consists of two stages. In the first stage of the initial analysis, the initial geostatic stress field is generated by defining the initial vertical stress distribution and coefficient of earth pressure at rest to auto generate the horizontal stress distribution. A body load is defined to bring the initial stress field to an equilibrium state without causing any mesh deformations. Then in the second stage, penetration of 10% of D is applied to the pipeline. In all subsequent remeshing analyses, this initial stage is used to bring mapped stresses (from the old mesh to the new mesh) to an equilibrium state, before applying the 10% of D as a displacement controlled boundary to the pipeline in the second stage of the analysis.

Table 1. Material properties

	Seabed	Pipeline
Unit weight, γ (kN/m^3)	20	
Elastic Modulus, E (MPa)	2.0	1x10^9
Poisson's ratio, v	0.3	0.3
Cohesion, c' (kPa)	5	
Friction angle, ϕ' (°)	20	
Permeability coefficient, k (m/s)	2x10^{-8}	

4 RESULTS

In this section, results from the LDFE analysis are validated against centrifuge test data (Dingle et al., 2008) and previous LDFE analysis results published by Wang et al. (2010). Although Wang et al. (2010) presented LDFE analysis results considering undrained behavior for seabed soil without considering pore pressure effects, a coupled analysis produces undrained penetration, if the adopted penetration rate is sufficiently fast. According to Finnie and Randolph (1994), $vD/c_v > 30$ is required to maintain undrained conditions around a penetrating surface footing, where v is the rate of penetration, D is the footing diameter and c_v is the coefficient of consolidation. If the same analogy is adopted for pipelines, the penetration rate of 1 mm/s selected in this study and the centrifuge test by Dingle et al. (2008)

also simulates undrained conditions. This justification makes it valid to compare results from this study with results from undrained analysis of Wang et al. (2010).

4.1 *Mesh sensitivity*

Before comparing results from this study with published data, a mesh sensitivity analysis was carried out to select the suitable element size for the pipeline and the surrounding soil. In the coarse mesh, both pipe and soil were modelled using CPE4 and CPE4P elements, respectively, with 0.2 m node spacing for the soil and 0.1 m node spacing for pipe. In the fine mesh, node spacing for both soil and pipe was selected as 0.1 m. The vertical penetration resistance, R_v, against vertical penetration depth, V, is shown in Figure 2. In Figure 2, dimensionless parameters are used similar to the centrifuge modelling results and LDFE analysis results presented by Dingle et al. (2008), and Wang et al. (2010), respectively. Dimensionless penetration depth is defined as V/D. Dingle et al. (2008), and Wang et al. (2010) computed dimensionless penetration resistance as R_v/Ds_{uo} in their undrained LDFE analysis, where undrained shear strength, s_{uo} at the depth of pipe invert is given by,

$$s_{uo} = s_{um} + kz \tag{1}$$

where, s_{um} = 2.3 kPa is the undrained shear strength at the mudline and k = 3.6 kPa/m is the rate of change of undrained shear strength over depth z measured from the ground surface. In this study, coupled analysis was carried out using the Mohr-Coulomb model. Hence, R_v was converted into a dimensionless term using yield stress, f_y at the invert of the pipe.

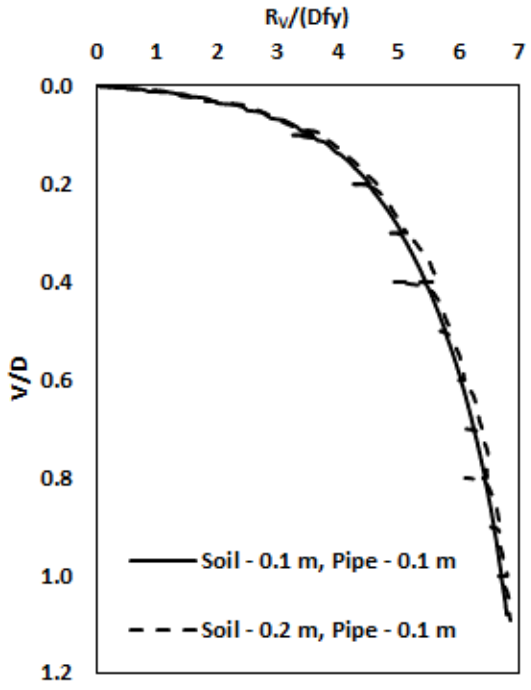

Figure 2. Vertical penetration resistance from fine and coarse meshes.

According to Figure 2, penetration resistance given by both fine and coarse meshes agree well. However, discontinuities observed after each remeshing step is more pronounced in the coarse mesh. Therefore, in what follows, fine mesh with node spacing of 0.1 m has been used.

4.2 *Comparison of vertical penetration resistance*

Figure 3 shows the vertical penetration resistance obtained from the proposed LDFE analysis for three cases: (i) pipe-soil interface is smooth, (ii) friction coefficient at the pipe-soil interface is 0.5 and the limiting shear stress is 2.5 kPa, which is half of c', and (iii) friction coefficient at the pipe-soil interface is 0.5 but there is no limiting shear stress. When the limiting shear stress is not defined, the limiting shear stress at the interface was computed by the contact algorithm for penalty method in ABAQUS/Standard as $\alpha\sigma_n$, where α is the friction coefficient at the interface and σ_n is the normal stress at the interface. Also in Figure 3, dimensionless penetration resistance obtained from the centrifuge test (Dingle et al., 2008) is presented.

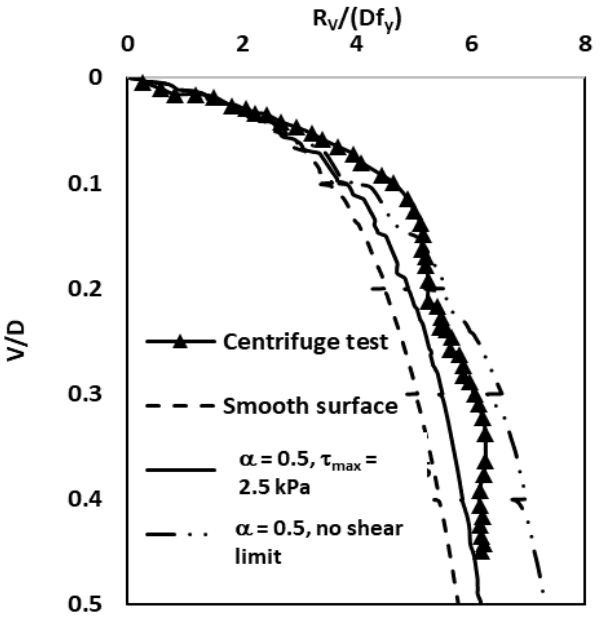

Figure 3. $R_v/(Df_y)$ from centrifuge and LDFE with different conditions at the pipe-soil interface.

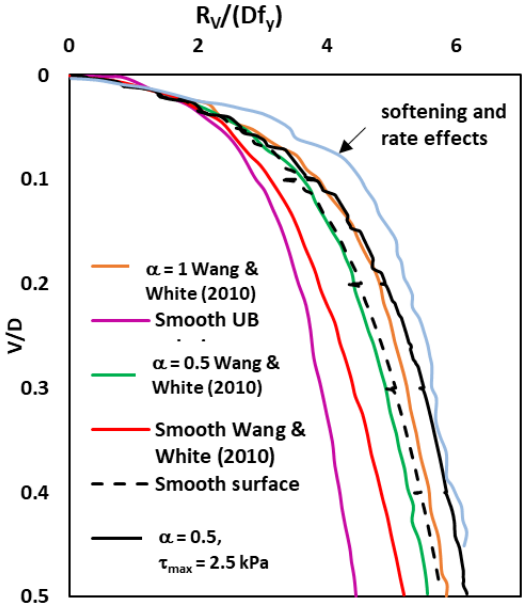

Figure 4. Comparison of LDFE with Wang et al. (2010), and UB (Randolph and White, 2008).

According to the results shown in Figure 3, it is clear that when the shear stress at the interface is limited, penetration resistance obtained from the remeshing analysis is smooth. When the interface is assumed perfectly smooth, predicted dimensionless

penetration resistance is at the lowest due to less resistance to soil flow at the pipe surface compared to the frictional interface. Other two cases with interface friction are not an exact match to the centrifuge test data, but close enough to say that both cases are in good agreement with centrifuge data.

A comparison of results from the proposed LDFE analysis and the LDFE analysis proposed by Wang et al. (2010) is shown in Figure 4. The major difference between the proposed LDFE approach and LDFE by Wang et al. (2010) for cases with no softening and no rate effects, is the pore pressure effects (considered in proposed approach) and the solution mapping from old mesh to new mesh (Wang et al., 2010 performed this outside ABAQUS using their own FOTRAN program based on Zienkiewicz and Zhu, 1992 patch recovery method). Despite these differences, two cases by Wang et al. (2010) with friction coefficients of 1 and 0.5 shows close agreement with results from the proposed approach when interface friction coefficient is 0.5 (with shear limit) or smooth. When the interface is smooth, Wang et al. (2010) produces lower penetration resistance than that obtained from the proposed approach. The difference between two approaches increased with increasing V, indicating that this difference may be due to the increased shear strength with dissipation of pore pressures in the proposed LDFE approach. Another contributing factor is the higher dimensionless submerged unit weight of soil ($\gamma' D/s_{um}$) used in this study, which is 4, compared to 2.26 used by Wang et al. (2010). With the increase in weight of the soil to be pushed upwards during pipe penetration, the force required to push the pipe in the downward direction increases. Due to the same reason, the Upper Bound solution by Randolph and White (2008) for the smooth interface and weightless soil shows the lowest penetration resistance.

4.3 *Soil flow around the pipe - Vertical penetration*

Figure 5 shows the soil flow around the pipeline obtained from the LDFE analysis for three penetration depths, V/D = 0.07, 0.25 and 0.35, same penetration depths as for the centrifuge test by Dingle et al. (2008). These flow patterns match closely with the those captured during the centrifuge test using the image analysis. Numerical results show fan shaped soil flow on either side of pipe invert at shallow embedment, forming the failure mechanism. With increasing embedment, fan shaped soil flow enlarges. At deeper embedment, soil underneath the pipe invert also contribute to the failure mechanism.

Although centrifuge tests by Dingle et al. (2008) show nonsymmetry in soil flow at deeper penetration depths, numerical results show symmetrical soil flow. The nonsymmetry in centrifuge tests may have caused due to a number of reasons: (i) nonhomogeneous nature of the soil and (ii) rotation or translation of the pipeline during vertical penetration. Although the free meshing technique used for mesh generation has not restricted the mesh to symmetry as shown in Figure 6, due to the uniform soil properties and symmetrical loading used in the numerical analysis, a symmetrical soil flow was generated around the pipeline.

4.4 *Pore pressure distribution and failure mechanism around the pipe*

Figure 6 shows the excess pore pressure distribution around the pipeline. The maximum excess pore pressure, 60 kPa, was observed at the vicinity of the pipe invert, which shows that significantly high excess pore pressures may generate during the vertical pipe penetration. Increasing excess pore pressures tend to reduce the shear strength closer to the pipe invert. Hence, soil below the invert has lower shear strength compared to the sides of the pipeline. According to Wang et al. (2010), softening due to accumulated plastic strains and rate effects must be included when simulating the pipeline penetration. In this study, softening due to accumulated plastic strains were not included. Nevertheless, good agreement between results by this study and centrifuge test was observed. The reason may be the reduced shear strength near the pipe invert incorporated in the coupled analysis. Hence one can argue that if a coupled analysis is considered, linking the yield strength of the soil to effective stresses, even an elastic perfectly plastic soil model such as Mohr-Coulomb has the ability to simulate the problem. The shear bands developed around the pipe shown in Figure 7 using LDFE analysis by Wang et al. (2010), considering softening and rate effects, and the proposed LDFE analysis further justifies the above statement.

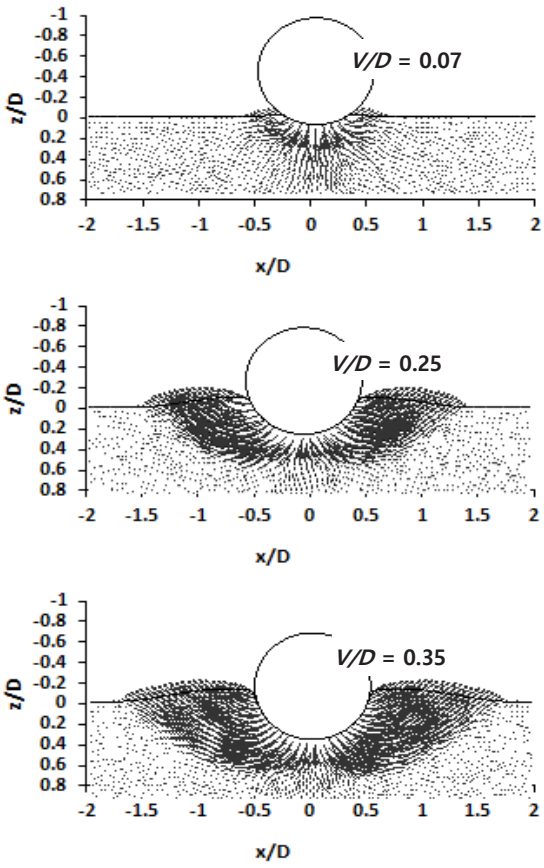

Figure 5. Soil flow around the pipeline.

4.5 *Lateral penetration*

During lateral penetration or breakaway of pipeline, it was restrained against vertical movement in this study. Also lateral penetration was carried out after pipe penetrated to a depth of D in the vertical direction. Both centrifuge test data and LDFE results from Wang et al. (2010) are not available for this case. Therefore, in this section, the observed soil flow around the pipe, the failure mechanism and penetration resistance from this study will be discussed.

Figure 8 shows the soil flow around the pipeline during the lateral movement. Soil is predominantly displaced in the lateral direction, but shows some movement in the upward direction towards the surface increasing the soil heave. Soil moving towards the surface rotates around the pipeline creating new contacts with pipe surface. Although soil movement around the pipeline is large, due to the remeshing approach adopted during the analysis has avoided mesh distortions as can be seen in Figure 9.

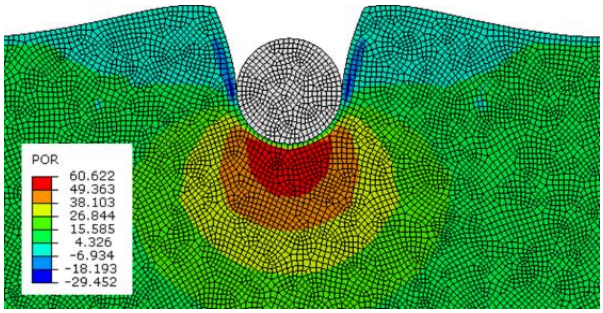

Figure 6. Pore pressure around the pipeline at the beginning of last remeshing analysis for vertical penetration.

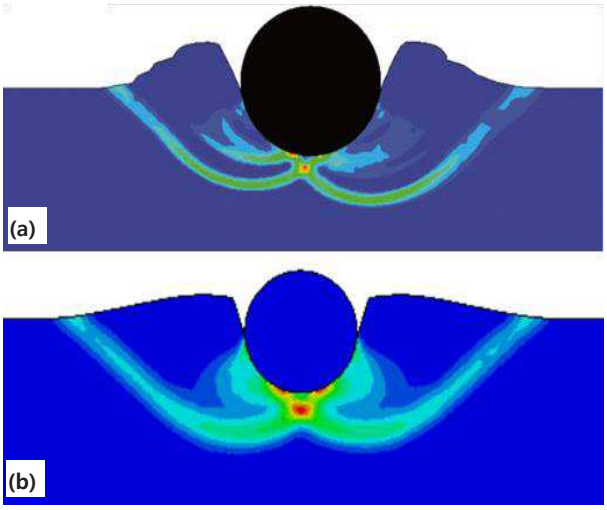

Figure 7. Shear band developed at vertical penetration of $D/2$ (a) Wang et al. (2010) and (b) proposed LDFE (Red to blue – Max to min plastic strain).

During vertical penetration, large excess pore pressures were generated below the pipe invert. However, during lateral penetration, excess pore pressures were not very high due the dissipation of excess pore pressures at the surface, which is close to the region of maximum excess pore pressure.

Figure 10 shows the penetration resistance during lateral penetration of the pipeline. Vertical penetration resistance, R_V, decreases rapidly during the first 0.1D of the lateral penetration and beyond that it shows a steady decline at a very slow rate. This is due to the loss of contact between rear of the pipeline and soil.

The lateral penetration resistance, R_H, also shows a rapid increase up to 0.1D but beyond that shows a steady increase at a very slow rate. The increase in R_H with increasing lateral pipe movement may be due to the formation of new contacts when soil pushed away in front of the pipe tends to rotate around the pipe towards the surface.

Figure 11 shows the development of failure mechanism during pure lateral translation of the pipeline considered in this study. This mechanism is similar to the one given by Randolph and White (2008) for pure translation. The size of the failure surface, which comprises of a fan shaped section and a linear surface, enlarges with increasing lateral pipe movement, U. The boundary of the fan shaped section is part of a circular arc. However, when the pipeline is free to move vertically during lateral translation, which resembles the practical situation in the field, the simple failure mechanism observed in this study may not be valid.

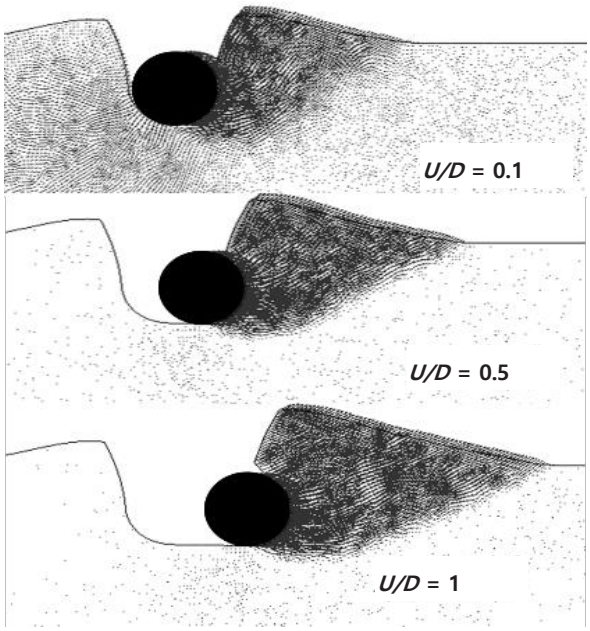

Figure 8. Soil flow around the pipeline.

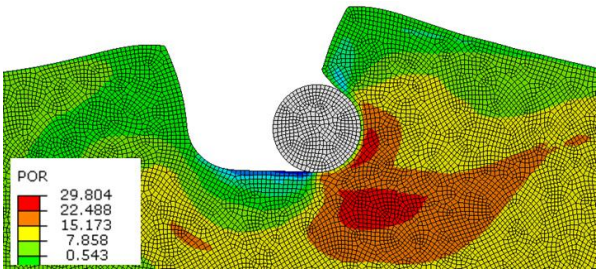

Figure 9. Deformed mesh and excess pore pressure distribution after lateral penetration of D.

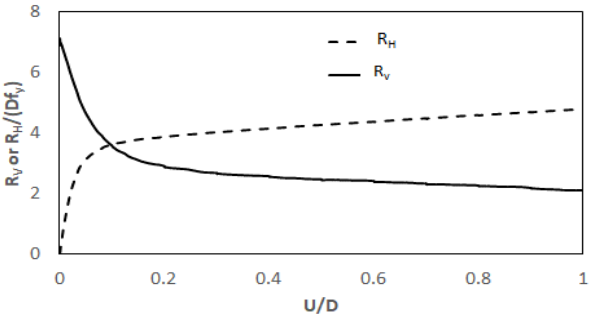

Figure 10. Horizontal, R_H, and vertical, R_V, penetration resistance during lateral penetration.

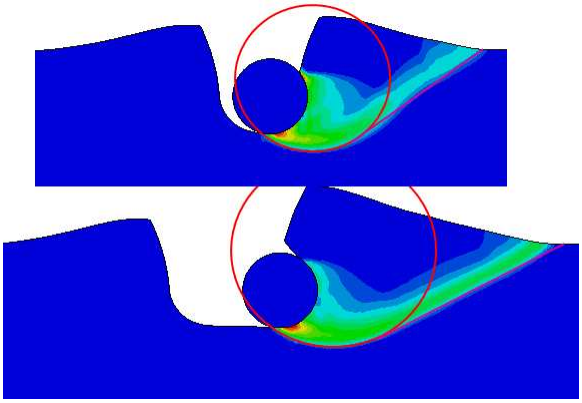

Figure 11. Failure mechanism evolving around pipeline during lateral movement.

5 CONCLUSIONS

In this paper, a remeshing and interpolation based coupled analysis technique developed within PYTHON Development Environment (PDE) in ABAQUS/Standard finite element program is presented. It has the ability to simulate deep penetration problems such as pipeline penetration and subsequent breakaway, which involves large soil deformations, otherwise impossible to simulate using finite element programs based on the small-strain approach. Vertical penetration resistance from the proposed LDFE analysis matches well with centrifuge test data and previous LDFE analysis results for undrained conditions by Wang et al. (2010) confirming that the proposed coupled LDFE approach is a useful tool in simulating deep penetration problems in geotechnical engineering.

6 REFERENCES

Aubeny, C.P., Shi, H. and Murff, J.D. (2005). Collapse loads for a cylinder embedded in trench in cohesive soil, *International Journal of Geomechanics*, Vol. 5, No. 4, pp. 320-325.

Chatterjee, S., Randolph, M.F. and White, D.J. (2012). The effects of penetration rate and softening on the vertical penetration resistance of seabed pipelines, *Geotechnique*, Vol. 62, No. 7, pp. 573-582.

Dingle, H.R.C., White, D.J. and Gaudin, C. (2008). Mechanics of pipe embedment and lateral breakout on soft clay, *Canadian Geotechnical Journal*, Vol. 45, pp. 636-652.

Finnie, I.M.S. and Randolph, M.F. (1994). Punch-through and liquefaction induced failure of shallow foundations on calcareous sediments. *In Proceedings of the 7th international Conference on the Behaviour Offshore Structures*, Mass., Pergamon, Vol. 1, pp. 217-230.

Martin, C.M. and Randolph, M.F. (2006). Upper bound analysis of lateral pile capacity in cohesive soil. *Geotechnique*, Vol. 56, No. 2, pp. 141-145.

Merifield, R. S., White, D. J. and Randolph, M. F. (2008). The ultimate undrained resistance of partially embedded pipelines. *Geotechnique*, Vol. 58, No. 6, pp. 461–470.

Merifield, R. S., White, D. J. & Randolph, M. F. (2009). Effect of surface heave on response of partially embedded pipelines on clay. J. Geotech. Geoenviron. Engng, ASCE, Vol. 135, No. 6, pp. 819-829.

Randolph, M.F. and White, D.J. (2008). Upper-bound yield envelopes for pipelines at shallow embedment in clay, *Geotechnique*, Vo. 58, No. 4, pp. 297-301.

Wang, D., White, D.J. and Randolph, M.F. (2010). Large-deformation finite element analysis of pipe penetration and large-amplitude lateral displacement, *Canadian Geotechnical Journal*, Vol. 47, pp. 842-856.

Zienkiewicz, O.C., and Zhu, J.Z. (1992). The superconvergent patch recovery and a posteriori error estimates. Part 1: The recovery technique. *International Journal for Numerical Methods in Engineering*, Vol. 33, No. 7, pp. 1331–1364.